Applied Energy Symposium 2020: Low carbon cities and urban energy systems
October 10-17, 2020
Paper ID: CUE2020-D-094

Multi-objective Optimization of a Wind-solar Microgrid System Based on the Improved NSGA-II Method

Zhang Bai[1*], Jiying chen[1], Shenghao Jiang[2], Yu Yuan[1], Wenxin Hu[1], Bo Zheng[1]

1 College of New Energy, China University of Petroleum (East China)
2 School of Applied Science, Harvard University

ABSTRACT

Distributed energy planning is a complex issue, and the non-dominated sorting genetic algorithm (NSGA-II) is widely employed for the system multi-objective optimization. This algorithm screens the intermediate population based on the fixed crowding distance principle, it does not consider the dynamic crowding change and cannot satisfy the diverse search requirements of solution space in different evolutionary periods. In this paper, an improved NSGA-II method based on dynamic crowding distance and information entropy is proposed. Then a case study of a wind-solar integrated microgrid system is implemented, by refereeing the local meteorological conditions and power loads in Yunnan of China, the renewable energy system under study is optimized in terms of the system energy efficiency, energy volatility and net present cost. Results indicate that the energy system achieves a lower cost after optimization by the improved NSGA-II method, and the matching degree of renewable energy generation and electricity demand is evidently enhanced which means a better system operation stability. Comparing to the general NSGA-II, the improved algorithm also has superiority in convergence speed, and the research findings provide an alternative method for optimizing the renewable microgrid system.

KEYWORDS: NSGA-II, wind-solar microgrid, dynamic crowding distance, information entropy, multi-objective optimization

NOMENCLATURE

Abbreviations	
CEL	Coefficient of Energy Loss
CHV	Coefficient of History Volatility
NPC	Net Present Cost

Symbols	
C	Cost
P	Power
T	Temperature
v	Velocity
η	Efficiency

1. INTRODUCTION

Microgrid is an energy system usually composed of diverse distributed power sources and loads, and has the capabilities for energy capture, supply and storage[1]. Compared to the large-scale power grid, the microgrid is regarded as a dispatchable unit that readily meets the power needs of the specific end-users, which contributes to alleviating the contradiction between the growing local energy demand and the traditional highly concentrated power generation. However, the intermittent characteristics of renewable energy cannot to be ignored, which causes the severe problems of poor energy reliability and low energy efficiency in distributed energy system. Therefore, the system optimization of microgrid is critical, the performances on system thermodynamics and economics should be comprehensively considered.

The present multi-objective optimization methods mainly have two categories[2]. The first one is to transform the sub-objective function into a compound function that contains all the sub-functions and corresponding weights. This solution achieves effective simplification, while the weighting and calculation process are much subjective, and requires more debugging time. The second method is based on the Pareto non-dominated solution theory, and find the Pareto optimal solution set for the multi-objective problem and then select the optimal solution from the set according to the requirements. There are many types of modern

Selection and peer-review under responsibility of the scientific committee of CUE2020

optimization algorithms [3], including the non-dominated sorting genetic algorithm (NSGA-II), particle swarm algorithm[4] and various bionic algorithms (e.g., ant colony, firefly, artificial fish) [5]. Among them, NSGA-II is one of the most popular, while it still has some shortages, such as, easily fall into the local optimum [6,7].

In order to increase the diversity of the Pareto solution set and enable to adapt different characteristics of the search space requirements, an improved non-dominated sorting genetic algorithm is proposed in this work by employing the dynamic crowding distance strategy, and uses the information entropy and student's t-distribution to improve the rationality and reliability of crossover and mutation. The advantages of the improved approaches in approximation and calculation speed are verified through the test functions.

In section 2, a typical wind-solar microgrid system as a constrained nonlinear multi-objective optimization case is developed and mathematically modeled, and an improved NSGA-II method is proposed in section 3. In section 4, based on a case study of a power community, the feasibility of the new optimization method is analyzed. Finally, the main conclusions are drawn in section 5.

2. MATHEMATICAL MODELING OF A MICROGRID SYSTEM

A typical wind-solar integrated microgrid system is employed for optimization and evaluation by using the improved NSGA-II method. As shown in Fig. 1, the photovoltaic (PV) cell and the wind turbine are consisted in this system, and the battery package as a storage unit is installed for overcoming the uncertainty of renewable energy, the surplus electricity will be stored and released during the insufficient conditions.

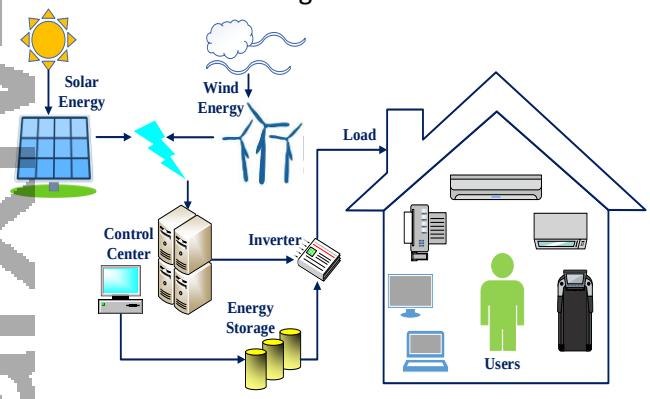

Fig. 1 Schematic of a typical wind-solar microgrid system

2.1 System mathematic model

2.1.1 Wind turbine power generation

The wind turbine with the nominal power capacity P_r of 1.5 MW is installed in this system, and the output power $P_{WT}(t)$ is a function of the wind velocity v below the height of wind turbine hub, as presented by Eq. 2-1:

$$P_{WT}(t)=\begin{cases}0, & v\le v_{\text{cut-in}} \text{ or } v\ge v_{\text{cut-out}}\\ P_r\left(\dfrac{v^3-v_{\text{cut-in}}^3}{v_r^3-v_{\text{cut-in}}^3}\right), & v_{\text{cut-in}}<v\le v_r\\ P_r, & v_r<v\le v_{\text{cut-out}}\end{cases} \quad (2\text{-}1)$$

where v_r, $v_{\text{cut-in}}$ and $v_{\text{cut-out}}$ are the rated rotating velocity (2.5m/s), switching-in velocity (18m/s) and cut-off rotating speed (12m/s), respectively.

2.1.1 Solar photovoltaic power generation

The installed PV module directly converts the solar irradiation into electric power $P_{PV}(t)$, which determined by the solar spectrum wavelength, absorptivity, aperture area and operation temperature, which can be modeled by Eq. 2-2:

$$P_{PV}(t)=\frac{G(t)}{1000}\times P_{\text{PV-STC}}\times r_{PV}\times[1-\beta_T(T_{PV}-T_{\text{PV,STC}})] \quad (2\text{-}2)$$

where $G(t)$ denotes the incident solar irradiation; $P_{\text{PV-STV}}$ and r_{PV} mean the PV rated power under the standard test condition (STC) and the PV power reduction coefficient, respectively; β_T is the PV temperature coefficient; $T_{\text{PV,STC}}$ and T_{PV} indicate the PV temperature at the STC and the PV operation temperature (as expressed by Eq. 2-3):

$$T_{PV}=T_{amb}+(NOCT-20)\times\frac{G(t)}{800} \quad (2\text{-}3)$$

where *NOCT* and T_{amb} are normal operating cell temperature of PV and the ambient temperature, respectively. The nominal power capacity is 0.325 kW with the PV efficiency of 16.94%.

2.1.3 Energy-storage subsystem: battery unit

A battery energy-storage system is used to minimize the imbalance between the power supply and demand in the microgrid system, and the battery status is determined by its charge or discharge operation, as presented in Eq. 2-4, and the battery input power will be positive or negative.

$$P_{batt}(t)=P_{WT}(t)+P_{PV}(t)-P_{load}(t)/\eta_{inv} \quad (2\text{-}4)$$

where $P_{batt}(t)$ and $P_{load}(t)$ are the instantaneous power loads of the battery and the end-user, η_{inv} denotes the inverter efficiency. Under the condition of $P_{BL}>0$ and $P_{BL}<0$, the battery unit will be charged or discharged. In this case, the state of charge (SOC) of the battery package is represented by Eq. 2- 5.

$$SOC_{batt}(t)=SOC_{batt}(t-1)\times(1-\sigma)\pm P_{batt\_load}\times\eta_b \quad (2\text{-}5)$$

where $SOC_{batt}(t)$ and $SOC_{batt}(t-1)$ mean the load status of the battery at the conditions of t and *t-1,* respectively;

η_b and σ are the efficiency and the self-discharge coefficient of the battery package, respectively. In this system, the designate capacity of the battery package is 167 A·h with the discharge and charge efficiencies of 85% and 95%, respectively.

2.2 System evaluation method

2.2.1 Energy Utilization Efficiency Index: Coefficient of Energy Loss (CEL)

In order to reduce the excessive power loss caused by overload power generation and improving the system energy utilization efficiency, it is necessary to evaluate the system's capability of utilizing renewable energy, and the coefficient of energy loss (CEL) is thereby used, as defined by the following:

$$P(t) = P_{\mathrm{WT}}(t)+P_{\mathrm{PV}}(t)+P_{\mathrm{batt}}(t) - P_{\mathrm{load}}(t) \tag{2-6}$$

$$\mathrm{CEL} = \frac{\sum_{t=1}^{n} \mathrm{Sign}(t) \times [P(t) - P_{\mathrm{batt}}(t-1)]}{\sum_{t=1}^{n} [P_{\mathrm{WT}}(t) + P_{\mathrm{PV}}(t)]} \tag{2-7}$$

where $P(t)$ represents the mismatch between the renewable power generation and the power load. Sign(t) is the sign function which indicates the energy storage condition.

2.2.2 Power Supply Stability Index: Coefficient of History Volatility (CHV)

For the purpose of efficiently utilizing the renewable sources of wind and solar energy, it is desired that the output power can be well matched and close to the consumption load, which contributes to avoiding the fluctuation of the entire system and improve the power supply quality. Thus, the system investigation on energy volatility is critical, including the backward and forward volatility. The power profile of the microgrid is a time series in nature, and the coefficient of history volatility (CHV) is thus proposed to evaluate the volatility of the energy system by referring the finical application, as follows:

$$u_t = \ln \frac{P(t)}{P(t-1)} \tag{2-8}$$

$$CHV = \sqrt{\frac{1}{n-1}\sum_{t=1}^{n} u_t^2 - \frac{1}{n(n-1)}\left(\sum_{t=1}^{n} u_t\right)^2} \tag{2-9}$$

2.2.3 Economic Index: Net Present Cost (NPC)

Another significant aspect is the system economic performance, the employed system net present cost (NPC) is defined as Eq. 2-10, and mainly consider the construction investment and the system operation & maintenance cost:

$$\begin{aligned} NPC &= C_{\mathrm{unit}} + C_{\mathrm{operation}} \\ &= (N_{\mathrm{wind}} \times C_{\mathrm{wind}} + N_{\mathrm{PV}} \times C_{\mathrm{PV}} + N_{\mathrm{batt}} \times C_{\mathrm{batt}}) + \\ &\quad (C_{\mathrm{OM\_wind}} \times t_{\mathrm{f}} + C_{\mathrm{OM\_PV}} \times t_{\mathrm{PV}} + C_{\mathrm{OM\_bat}} \times t_{\mathrm{batt}}) \end{aligned} \tag{2-10}$$

where C_{wind}, C_{PV} and C_{batt} represents the specific capital cost for PV module, wind turbine and energy storage battery, respectively; N_{PV}, N_{wind} and N_{batt} are the corresponding installed capacity; C_{OM} means the corresponding annual operation & maintenance cost.

2.3 System Constraints

Regarding to the evaluation and optimization of a wind-solar microgrid system, the local meteorologic condition of Yunnan, China will be considered, and the power capacity of this employed mircogrid case (will be detailedly introduced in Section 4) is approximate 2200 kW. Meanwhile, the constraints for system multi-objective optimization including the configuration constraint and system characteristic constraint, the former one is the configuration constraint which mainly consider the system installment, as the presented in Eq. 2-11.

$$\begin{cases} 0 \le N_{\mathrm{WT}} \le N_{\mathrm{WT\_max}} \\ 0 \le N_{\mathrm{PV}} \le N_{\mathrm{PV\_max}} \ , \ N_{\mathrm{WT}}, N_{\mathrm{PV}}, N_{\mathrm{batt}} \in N \\ 0 \le N_{\mathrm{batt}} \le N_{\mathrm{batt\_max}} \end{cases} \tag{2-11}$$

where $N_{\mathrm{WT\_max}}$, $N_{\mathrm{PV\_max}}$, $N_{\mathrm{batt\_max}}$ are the maximum installment of wind turbines, photovoltaic modules and battery package, respectively, and these device constraints will be correspondingly set as 10, 20000 and 500, respectively.

While the system characteristic constraint is mainly referring the microgrid matchment on power supply and demand, and the allowed maximum energy shortage ratio R of this system is used to represent the system reliability, as Eq. 2-12:

$$R < \sum_{t=1}^{8760} P_{t\_\mathrm{shortage}} \Big/ \sum_{t=1}^{8760} P_{t\_\mathrm{load}} \tag{2-12}$$

where P_{t_shortage} is the hourly generated renewable power when occur the power shortage. Regarding to the off-grid system, R should be equal to 0.

3. IMPROVED NSGA-II METHOD OF OPTIMIZATION

The multi-objective optimization solution of the microgrid need simultaneously optimizing all the referred objective functions, including the aspects of economy, energy efficiency and operation stability. NSGA-II, as one of the most commonly used optimization methods, lacks of enough diversity of the

Pareto solution set, and the traditional crossover operator cannot adapt to the different characteristics of the search space requirements. Therefore, an improved NSGA-II method is developed in this work, and the following achievements are obtained.

3.1 Dynamic Crowding Distance

In order to comprehensively consider the changes of crowding distance for neighboring individuals within the screening process[8], this work adopts the principle of dynamic crowding distance during calculation. And summarized as follows: (1) calculate the initial crowding distance of several solutions; (2) delete the solution with the smallest crowding distance; (3) record the position of the deleted solution; (4) update the crowding distance in the neighborhood and delete the smallest congestion after completing the update. When the number of solutions is equal to the number of required individuals to enter the next evolution, stop the screening process.

3.2 Calculation Operator Improvement

The occurrence of crossover and mutation can be regarded as random variables, and the random variable uncertainty measurement function has a unique form[8]:

$$H(X) = -C\sum_{x=1}^{i} p(x)\log_2 p(x) \tag{3-1}$$

The information entropy is employed to represent the uniformity of the individual in the solution space, And the preliminary setting forms of the crossover and mutation probability are expressed by Eqs. 3-2 and 3-3 respectively.

$$P_{c1} = k_1(1-\frac{i}{N}) \qquad (i < N) \tag{3-2}$$

$$P_{m1} = k_2(1-\frac{i}{N}) \qquad (i < N) \tag{3-3}$$

where k_1 and k_2 are the constants that above 0 and below 1, respectively. N is the total number of individuals in the population, i is the number of individuals in a certain evolutionary stage, and a smaller i means a greater genetic probability with a more stable population structure [9].

In the initial stage of population evolution, the similarity of population individuals is low, increasing the crossover probability will accelerate the evolution of the population, meanwhile reducing the mutation probability of the population can reduce the tedious calculation process. During the middle stage of the evolution, appropriately increasing the mutation probability will effectively prevent the algorithm iteration from falling into the local optimum. At the end of the evolution, the individual similarity is high. While the crossover probability and mutation probability should be reduced for achieving the algorithm converge gradually, in addition, in order to realize the aforementioned optimization thoughts, the improvements of the calculation operators are formulated as follows:

$$P_c = k_1 - \frac{k_1 m}{N} + k_3 e^{-\frac{t}{T_{\max}}} \tag{3-3}$$

$$P_m = k_2 - \frac{k_2 m}{N} + k_4 \frac{\Gamma\left(\frac{n+1}{2}\right)}{\Gamma\left(\frac{n}{2}\right)\sqrt{n\pi}}\left(1+\frac{(\frac{t-T/2}{k_4})^2}{n}\right)^{-\frac{n+1}{2}} \tag{3-4}$$

In the process of crossover calculation, a decreasing function in the range of 0 to 1 is introduced, and the student's t-distribution is applied to simulate the dynamic demand of mutation probability. The parameter of n means the freedom degree, as expressed in Eq. 3-5, when n tends to infinity, the t-distribution will be a standard normal distribution.

$$n = \left[k_5 \exp(t - k_6 T_{\max})\right] + 1 \tag{3-5}$$

where $T_{\max}$ is the maximum evolutionary generations. In this work, the values of k_5 and k_6 are 99 and 0.5, respectively. At the beginning of generations, the value of n is approximately 1, and the t-distribution is Cauchy distribution. When the evolutionary generations reach a half of $T_{\max}$, the corresponding t-distribution will be laid between the Cauchy and the normal distributions. Selecting ZDT1 and ZDT2 as the algorithm test examples, each test function is run 10 times and recorded the average value, and the convergence criterion (γ) and running time (RT/s) are selected as evaluation criteria. Compared to the general NSGA-II, the improved NSGA-II algorithm has better convergence and running speed, as shown in Table 1 and Fig. 2, and the optimized solution set is closer to the real Pareto frontier.

Table 1 Test Functions Details and Evaluation Results

	Definition	Constraints	Index	General NSGA-II	Improved NSGA-II
ZDT1 Pareto Convex	$f_1(x) = x_1$ $f_2(x) = g(x)(1-\sqrt{\frac{x_1}{g(x)}})$ $g(x) = 1+9/(n-1)\cdot\sum_{i=2}^{n} x_i$	n=30 $x_i \in [0,1]$	γ RT/s	0.0150 22.9	0.0142 20.5
ZDT2 Pareto Concave	$f_1(x) = x_1$ $f_2(x) = g(x)[1-(\frac{x_1}{g(x)})^2]$ $g(x) = 1+9/(n-1)\cdot\sum_{i=2}^{n} x_i$	n=30 $x_i \in [0,1]$	γ RT/s	0.0133 25.4	0.0128 21.2

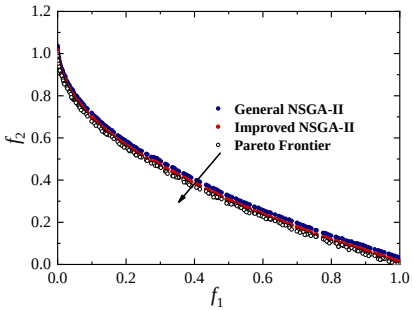

Fig. 2 Comparison of the general/improved NSGA-II and the real Pareto Frontier

4. CASE STUDY OF MICROGRID SYSTEM

In this work, a wind-solar microgrid system will be optimized based on the improved NSGA-II method, and a small size power community is set as an end power consumer, which including an industrial park, three shopping malls and ten residential communities, located in Yunnan, China. The hourly-step power load of users is also simulated, as shown in Fig. 3.

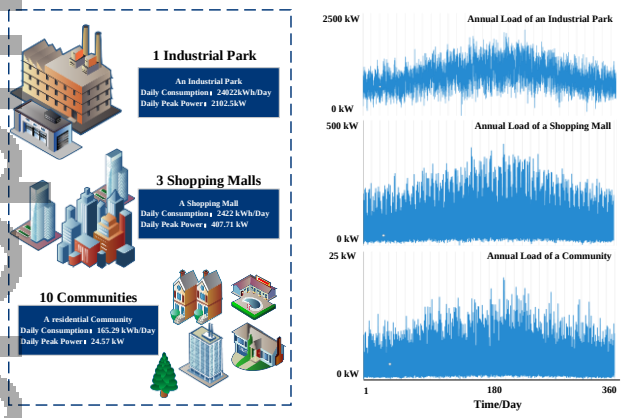

Fig. 3 Component of the end-user and the power profiles

The mentioned power user has a quite different characteristic, the electricity consumption of industrial parks is dominant, while the shopping mall and residential communities have their own daily fluctuation characteristics which represent the preferences of human activities.

The local meteorological condition is significant, and directly affect the power generation by the wind turbine and PV, the local statistically averaged wind speed and solar irradiation are summarized in Fig. 4.

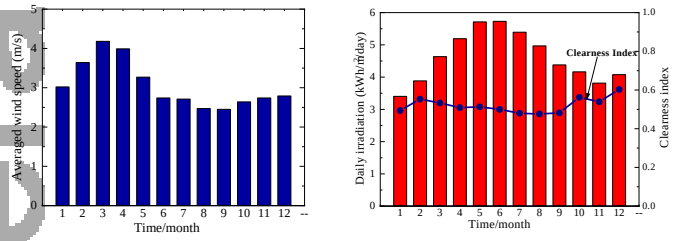

Fig. 4 Statistical wind speed and solar irradiation

The newly developed improved NSGA-II method is used to optimize this renewable microgrid, and the algorithm flow is shown in Fig. 5.

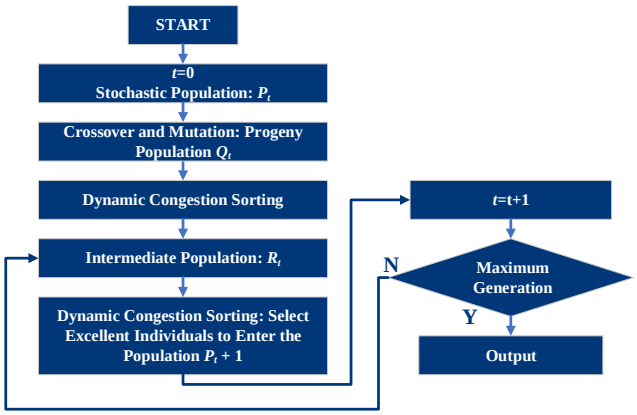

Fig. 5 Flow Chart of Improved NSGA-II

The set multi-objective functions for optimization including the system annual net present cost, average historical volatility and energy loss coefficient, the convergence of the algorithm is analyzed with the evaluation index system proposed in this paper, and the results are shown in Fig. 6.

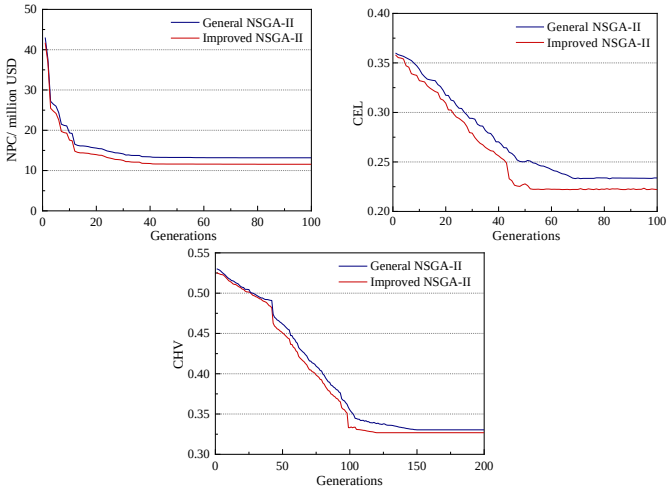

Fig. 6 Results comparison of general and Improved NSGA-II

Through comparison, the optimization of the improved algorithm achieves evidently enhancement. The NPC realizes a further reduction of 7.57% by the improved NSGA-II optimization. Meanwhile, CEL is decreased to 0.22 from 0.32, which means a better matching degree between the load and the renewable power output, additionally, the favorable complementary of wind and solar energy is achieved with CHV reduced to 0.326. In addition, compared to the general NSGA-II, the improved algorithm has a faster converge speed, and the converge generations for optimization of CEL and CHV are 70th and 50th , respectively, while the corresponding generation algorithm need 150th and 100th.

5. CONCLUSION

In this work, an improved NSGA-II multi-objective optimization algorithm is developed to further enhance the optimization of renewable microgrid system, and the main research findings can be outlined as follows:

(1) A new operator improved by information entropy and student's t-distribution is proposed in the improved NSGA-II method. Through the test functions, the rationality of the improved measures is verified.

(2) The mathematic model of a wind-solar microgrid system is developed and a comprehensive evaluation model, including net present cost, historical volatility and energy loss coefficients are also proposed.

(3) Through the multi-optimization by the improved NSGA-II method, an effective improvement on convergence characteristics is achieved, moreover, the optimized functions of NPC, CEL and CHV on the evaluated microgrid system realize further reduction.

The research findings test the feasibility of the newly developed optimization algorithm, and provides an alternative way to enhance the complementary of renewable energy for distributed energy supply.

ACKNOWLEDGEMENT

The authors appreciate the financial support provided by the National Natural Science Foundation of China (No. 51706249) and the Fundamental Research Funds for the Central Universities (No. 19CX05002A).

REFERENCE

[1] Habib HF, Lashway CR, Mohammed OA. A Review of Communication Failure Impacts on Adaptive Microgrid Protection Schemes and the Use of Energy Storage as a Contingency. IEEE T Ind Appl 2018; 54(2): 1194-1207.

[2] Dou C, Zhou X, Zhang T, Xu S. Economic optimization dispatching strategy of microgrid for promoting photoelectric consumption considering cogeneration and demand response. J Mod Power Syst Cle 2020; 8(3): 557-563.

[3] Zhou YT, Wang YN, Wang K, Kang L, Peng F, Wang LC, Pang JB. Hybrid genetic algorithm method for efficient and robust evaluation of remaining useful life of supercapacitors. Appl Energ 2020;260114169.

[4] Ray PK , Mohanty A . A robust firefly – swarm hybrid optimization for frequency control in wind/PV/FC based microgrid. Appl Soft Comput 2019; 85, 105823.

[5] Guo J, Zhong J, Li Y. A hybrid artificial fish swam algorithm for disassembly sequence planning considering setup time. Assembly Autom 2019, 39(1): 140-153.

[6] Swain KP, De M. DSM for all-day voltage profile improvement in a microgrid. IET Renew Power Gen 2019; 13(6):990-997.

[7] Mokhtari Y, Rekioua D. High performance of Maximum Power Point Tracking Using Ant Colony algorithm in wind turbine. Renew Energ 2018, 126:1055-1063.

[8] Chen L, Li Q, Zhao X, et al. Multi-population coevolutionary dynamic multi-objective particle swarm optimization algorithm for power control based on improved crowding distance archive management in CRNs. Comput Commun 2019, 145:146-160.

[9] Dong X, Qian M, Jiang R. Packet classification based on the decision tree with information entropy. J Supercomput 2020, 76(6): 4117-4131.